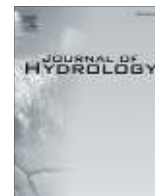


Contents lists available at ScienceDirect

Journal of Hydrology

journal homepage: [www.elsevier.com/locate/jhydrol](http://www.elsevier.com/locate/jhydrol)

## Interaction of a river with an alluvial basin aquifer: Stable isotopes, salinity and water budgets

Christopher J. Eastoe<sup>a,\*</sup>, William R. Hutchison<sup>b</sup>, Barry J. Hibbs<sup>c</sup>, John Hawley<sup>d</sup>, James F. Hogan<sup>e</sup>

<sup>a</sup>SAHRA/Department of Geosciences, University of Arizona, Tucson, AZ 85721, USA

<sup>b</sup>Texas Water Development Board, P.O. Box 13231, Austin, TX 78711-3231, USA

<sup>c</sup>CEA-CREST/Dept. of Geological Sciences, California State University-Los Angeles, Los Angeles, CA 90032-8203, USA

<sup>d</sup>Hawley Geomatters, P.O. Box 4370, Albuquerque, NM 87196, USA

<sup>e</sup>SAHRA, University of Arizona, Tucson, AZ 85721, USA

### ARTICLE INFO

#### Article history:

Received 12 June 2009

Received in revised form 27 July 2010

Accepted 6 October 2010

Available online xxxxx

This manuscript was handled by L. Charlet, Editor-in-Chief, with the assistance of Tamotsu Kozaki, Associate Editor

#### Keywords:

Groundwater

Recharge

Stable isotopes

Salinity

MODFLOW

Groundwater budgets

### SUMMARY

Detailed sets of tracer data (isotopes, salinity) and the results of MODFLOW modeling of water budgets provide an unprecedented opportunity for comparing modeling with field data in the area where the Rio Grande enters the Hueco Bolson basin of Texas and Chihuahua. Water from the Rio Grande has recharged the Hueco Bolson aquifer to a depth of 300 m below the surface in the El Paso-Ciudad Juárez area, the depth of infiltration corresponding to the depth of ancestral Rio Grande fluvial sediments. Groundwater beneath the river exhibits complex isotope and salinity stratification. Post-dam (post -1916, type A) river water has infiltrated to depths up to 80 m. Pre-dam (type B) river water has infiltrated to 300 m depth near downtown El Paso, and has mixed with, or been displaced further downstream by high-salinity native Hueco Bolson groundwater (type C, present in the basin north of the river). Salinity and isotope boundaries do not correspond precisely. Isotope stratification corresponds to water residence time and (for type C) to degree of evaporation; the highest salinities are associated with the most evaporated water. Modeling of water budgets in the basin fill beneath the river predicts present-day mixing of water types B and C where changing rates of pumping have caused a reversal of groundwater flow direction between El Paso and Ciudad Juárez, and deep recharge of type B water under conditions prevailing in the 1960s.

© 2010 Elsevier B.V. All rights reserved.

### 1. Introduction

Interactions between surface water and groundwater are potentially complicated near the point of entry of a river into an alluvial basin, particularly if the basin aquifers have been heavily pumped for decades. MODFLOW modeling, based on aquifer properties and depths to water in observation wells, provides “snapshot” pictures of groundwater flow conditions at chosen times for which input data are available. It is instructive to compare model output with tracer data, which provide a picture of the integrated effects of flow over a prolonged time interval. Stable O and H isotope and salinity data are rarely available in sufficient detail to depict the vertical dimension of aquifers beneath a river in a useful fashion. Where suitable isotope and salinity distinctions exist, they can be used to map the distribution of water types, to indicate zones of recharge and discharge, and to demonstrate the effects of pumping.

Such data are not usually available in detail, particularly in the vertical dimension, for several reasons, e.g.: the prohibitive cost of drilling test holes with discrete vertical zone sampling; the long screened intervals of supply wells; and the lack of supply wells in saline domains of an aquifer.

The interaction of groundwater from the regional Hueco Bolson aquifer of Texas and Chihuahua and river water from the Rio Grande can be examined in detail, thanks to a coupled drilling and flow modeling project undertaken in 2002 and 2003 by the city of El Paso, Texas. The investigative drilling program included several test holes penetrating the Hueco Bolson aquifer beneath the Rio Grande to depths ranging to 360 m. Discrete vertical zone sampling provided an opportunity to map the “stratigraphy” of the aquifer in terms of isotopes and salinity. A concurrent, but independent, MODFLOW modeling study allowed for comparison of the observed “stratigraphy” with calculated water budgets and implied flow directions.

The area (Fig. 1) is of considerable interest because it lies along the border between the USA and Mexico, and within a metropolitan area, El Paso, Texas and Ciudad Juárez, Chihuahua, with a combined population exceeding 2 million. Continuing urban population

\* Corresponding author. Tel.: +1 520 621 1638; fax: +1 520 621 2672.

E-mail addresses: [eastoe@email.arizona.edu](mailto:eastoe@email.arizona.edu) (C.J. Eastoe), [bill.hutchison@twdb.state.tx.us](mailto:bill.hutchison@twdb.state.tx.us) (W.R. Hutchison), [bhibbs@exchange.calstatela.edu](mailto:bhibbs@exchange.calstatela.edu) (B.J. Hibbs), [jgeomatters@qwest.net](mailto:jgeomatters@qwest.net) (J. Hawley), [jfhsnm@gmail.com](mailto:jfhsnm@gmail.com) (J.F. Hogan).

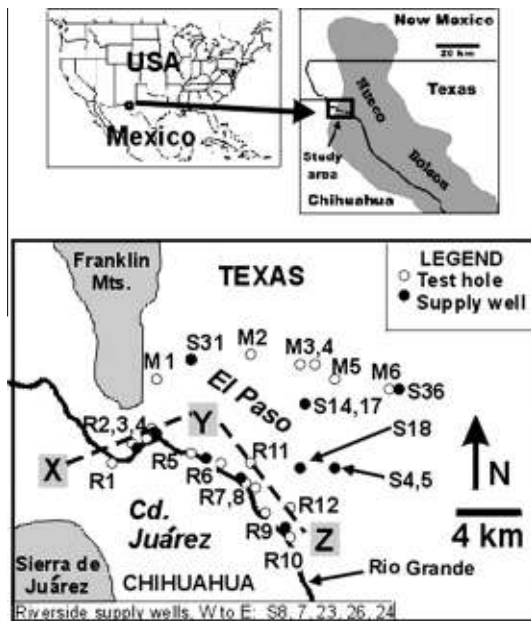


Fig. 1. Location map based on Landsat image of El Paso and Ciudad Juárez. The Rio Grande is the international boundary between the US and Mexico. The map shows test hole locations (R1–12 in the flood plain traverse; M1–6 in the mesa traverse) and municipal supply wells labeled Sx. X, Y and Z give the location of the vertical section of Fig. 2.

growth raises concerns about future water supply and the need for a thorough understanding of the subjacent aquifers. Decades of municipal pumping have greatly modified both the shallow alluvial aquifer beneath the Rio Grande (Hutchison and Hibbs, 2008) and the regional Hueco Bolson aquifer (Hibbs et al., 1997), leading to likely changes in flow direction (Hutchison and Hibbs, 2008), and to salinity increases (Hibbs et al., 1997).

Further interest is generated by the presence of the Elephant Butte dam on the Rio Grande in New Mexico, 255 km upstream of El Paso. The dam, which impounds a large reservoir, was completed in 1916. El Bakri et al. (1992) and Eastoe et al. (2008) documented the stable O and H isotope effect of large dams. Eastoe et al. (2008) demonstrated the isotope distinction between pre-dam and post-dam river water now present as groundwater in the Hueco Bolson aquifer, and suggested that that distinction could serve locally as a tool for dating groundwater. The flood plain of the Rio Grande in the Hueco Bolson is a suitable study area in which to test this suggestion.

In this article, we present isotope and salinity data for water in two vertical sections in the urban part of the Hueco Bolson: one beneath the Rio Grande and another more than 5 km north of the river. We also present flow budgets determined from MODFLOW modeling for the aquifers beneath the Rio Grande flood plain. Hutchison and Hibbs (2008) provided a regional context by relating isotope data from supply wells and MODFLOW modeling at a scale of tens of km, deducing large-scale movements of groundwater and the effects of pumping. In the more limited area near the entry point of the river into the Hueco Bolson, the present study makes use of highly detailed tracer data sets with ~1 km resolution in the horizontal dimension and better than 30 m resolution in the vertical dimension, and MODFLOW modeling and a newly-available geological section at similar scales. The principal focus is the comparison of model results with detailed field data in unprecedented detail, and an examination of the complementary roles of two views of groundwater interaction beneath the river, one from tracer data, and the other from flow modeling. In addition, we examine: 1. The relationship of groundwater beneath the river with that from the basin north of the river; 2. The use of the dam-related isotope

effect as a local dating tool; 3. The evidence for deep infiltration of river water, in relation to basin geology.

## 2. Study area

### 2.1. Geology

The study area lies within the Hueco Bolson, one of several fault-bounded basins making up the Rio Grande Rift within the Basin and Range province of western North America. The Basin and Range province consists of numerous fault-bounded basins filled with Neogene alluvium and separated by mountain ranges of pre-Neogene crystalline rock. The Hueco Bolson is an asymmetric graben, 330 km long and up to 55 km wide, with the largest displacement and the deepest alluvium (>2700 m; Collins and Raney, 1994) along faults on the western margin, next to the Franklin Mountains. Basin fill consists of alluvial, fluvial and lacustrine sediments associated with the Neogene Santa Fe Group (Hawley and Kernodle, 2000). In the study area, the upper 500 m of the Santa Fe Group comprise lacustrine sediment (Middle Santa Fe Group, locally called the Fort Hancock Formation) overlain by largely fluvial sediment (Upper Santa Fe Group, locally called the Camp Rice Formation); both formations include alluvium derived from the mountains to the west (Fig. 2). The evolution of the sedimentary facies corresponds to a transition from a closed lacustrine basin in the Pliocene to the present basin in which the upper and lower Rio Grande drainage systems have been integrated (Stuart and Willingham, 1984; Connell et al., 2005). The ancestral Rio Grande followed the east side of the Franklin Mountains and the Sierra de Juárez during the early and middle Pleistocene, depositing the Camp Rice Formation in a basin deepened on the west side by subsidence along the range-bounding fault. Since the late Pleistocene (670,000 years ago), the Rio Grande has followed its present course, entering the Hueco Bolson through a canyon between the Franklin Mountains and the Sierra de Juárez (Stuart and Willingham, 1984). Recent alluvium underlies the present flood plain to a maximum depth of 60 m.

### 2.2. Hydrogeology

A brackish shallow alluvial aquifer occurs within 30 m of the surface of the present flood plain of the Rio Grande. At present, Rio Grande water infiltrates into the alluvial aquifer in the study area as a result of pumping, which has in places reversed the pre-development vertical gradient between the river and aquifer (Hutchison and Hibbs, 2008). The deeper, regional Hueco Bolson aquifer is present below the alluvial aquifer, and at depths below 80 m from the surface of the mesas north of the Rio Grande. The Hueco Bolson aquifer discharged to the alluvial aquifer prior to development in the eastern part of the study area (Hutchison and Hibbs, 2008). Water in the upper parts of the Hueco Bolson

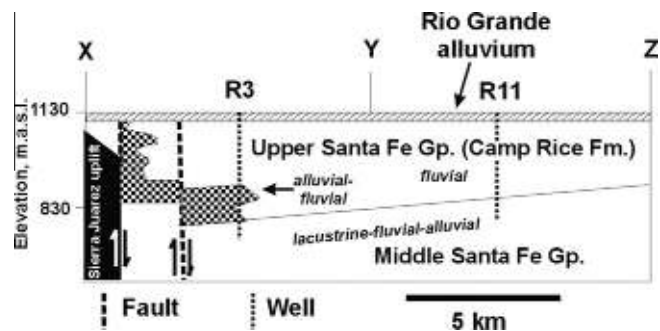


Fig. 2. Vertical section of the field area (see Fig. 1 for location), showing geology, and locations of test holes R3 and R11.

**Table 1**  
Isotope and specific electric conductivity data.

Site Date	Depth, m Upper	Depth, m Lower	$\delta^{18}\text{O}$ (‰)	$\delta\text{D}$ (‰)	EC ( $\mu\text{S}/\text{cm}$ )	Site Date	Depth (m) Upper	Depth (m) Lower	$\delta^{18}\text{O}$ (‰)	$\delta\text{D}$ (‰)	EC ( $\mu\text{S}/\text{cm}$ )
<i>River section</i>											
R1 (Chihuauita)	97.0	100.0	−9.3	−76	2340	R4 (Bowie High Sch.)	71.2	74.2	−10.7	−82	
	130.3	133.3	−10.1	−79	2880		89.4	92.4	−10.7	−84	1550
	154.5	157.6	−10.9	−85	1990		121.2	124.2	−10.9	−85	1710
December-2002	181.8	184.8	−10.9	−84	1820		160.6	163.6	−11.1	−86	940
	206.1	209.1	−11.0	−86	1380	December-2002	192.4	195.5	−11.0	−87	800
	219.7	222.7	−11.3	−87	880		218.2	221.2	−11.3	−87	640
	250.0	253.0	−9.6	−72	10,560		253.0	256.1	−10.9	−84	1020
	272.7	275.8	−9.8	−72	11,430		272.7	275.8	−10.9	−84	1100
	297.0	300.0	−9.6	−72	12,589		298.5	301.5	−10.7	−82	1330
	309.1	312.1	−9.7	−73	13,800		318.2	321.2	−10.4	−77	6400
	318.8	321.8	−9.6	−71	14,520		333.3	336.4	−10.8	−77	6490
R2 (TH17A)	65.2	68.2	−10.3	−77	4865	R5 (LVTP-2003)	51.5	45.5	−8.4	−70	1443
	101.5	104.5			1540		72.7	66.7	−8.3	−70	1458
	122.7	125.8	−10.7	−82	1850		125.8	119.7	−10.5	−83	1790
November-2002	163.6	166.7	−9.2	−75	4860	August-2003	177.3	171.2	−10.9	−83	2380
	180.3	183.3	−10.0	−79	4780		224.2	230.3	−10.3	−80	3170
	203.0	206.1	−10.8	−83	3070		245.5	251.5	−10.2	−77	2070
	219.7	222.7	−10.8	−83	2420		268.2	274.2	−10.2	−73	9490
	245.5	248.5	−11.1	−87	890		316.7	322.7			1226
	263.6	266.7	−10.6	−80	740		347.0	353.0			6380
	284.8	287.9	−11.2	−88	770		25.8	31.8	−6.8	−61	1606
	304.5	307.6	−11.2	−86	930	R6 (LVTP-04)	60.6	66.7	−7.5	−65	1804
R3 (TH14A)	85.8	88.8	−10.7	−83	1906		100.0	106.1	−10.1	−79	3330
	95.5	98.5	−10.6	−83	1952	July-2003	172.7	178.8	−10.2	−76	3410
	124.2	127.3	−10.7	−86	1047		200.0	10.1	−10.1	−74	1646
December-2002	136.4	139.4	−10.1	−85	1830		225.8	231.8			1104
	227.3	232.7	−11.1	−86	908		243.9	250.0			2290
	253.0	256.1	−11.1	−86	1650		287.9	293.9	−10.2	−75	2540
	274.2	277.3	−10.3	−80	1577						
	286.4	289.4	−10.9	−85	1699	R7 (LVTP-05)	45.5	51.5			1825
	309.1	312.1	−10.5	−73	14,200		62.1	68.2			1714
	360.6	363.6	−10.0	−76	25,500		78.8	84.8			2070
R7 (LVTP-05)	112.1	118.2			2320	R9 (LVTP-08)	175.8	181.8	−10.5	−76	1866
	142.4	148.5			1956		222.7	228.8	−10.2	−73	10570
	166.7	172.7			1284		295.5	301.5	−9.8	−71	16850
July-2003	207.6	213.6			3650						
	242.4	248.5			7650	R10 (LVTP-10)	78.8	84.8	−10.6	−81	2880
	300.0	306.1			14,450		133.3	139.4	−10.1	−78	2040
							184.8	190.9	−10.5	−76	6790
R7 (USGS)		11.5	−7.2	−66		June-2003	216.7	222.7			10,790
		37.6	−8.0	−70			265.2	271.2	−9.9	−72	19,220
		57.9	−8.3	−71			300.0	306.1	−9.4	−70	30,600
July-2002		108.5	−9.8	−76							
		174.5	−10.3	−77		R11 (LVTP-06)	43.9	37.9	−8.9	−70	3370
		202.7	−10.7	−76			75.8	69.7	−9.1	−71	3810
							109.1	103.0	−9.6	−72	2430
R8 (LVTP-07)	24.2	30.3	−8.2	−70	1657	August-2003	151.5	145.5	−10.1	−75	1034
	36.4	42.4	−7.9	−70	1701		181.8	175.8	−9.1	−69	5400
	51.5	57.6	−8.1	−70	1493		203.0	197.0	−10.7	−77	3330
June-2003	75.8	81.8	−9.8	−72	2860		230.3	224.2	−10.5	−77	5200
	109.1	115.2	−10.1	−75	1449		265.2	259.1	−10.4	−75	10,700
	133.3	139.4	−10.3	−77	2030		3327.3	327.3	−10.2	−73	14,610
	172.7	178.8	−10.3	−77	3780						
	225.8	231.8	−10.0	−74	8620	R12 (LVTP-09)	42.4	48.5	−8.1	−70	2730
	281.8	287.9	−9.7	−72	13,600		69.7	75.8	−8.3	−70	2050
							97.0	103.0	−10.3	−76	1737
R9 (LVTP-08)	39.4	45.5	−7.8	−69	1468	July-2003	121.2	127.3			2490
	57.6	63.6	−7.9	−68	1475		154.5	160.6	−10.8	−77	5430
	72.7	78.8	−8.1	−69	1470		200.0	206.1	−10.4	−75	10,910
June-2003	78.8	84.8	−7.9	−70	1474		224.2	230.3	−10.4	−74	14,360
	90.9	97.0	−9.6	−76	2250		248.5	254.5	−10.0	−72	17,670
	124.2	130.3	−9.9	−76	3080		284.8	290.9	−10.0	−72	18,740
<i>Mesa section</i>											
M1 (PTWF-04)	119.7	125.8	−9.3	−64	4380	M1 (PTWF-04)	398.5	404.5	−10.5	−75	2490
	153.0	159.1	−9.4	−66	47.0		447.0	153.0	−10.6	−74	4880
	181.8	187.9	−9.6	−67	498						
August-2003	206.1	212.1	−9.1	−63	581	M2 (TH76A)	163.6	169.7	−9.8	−70	690
	254.5	260.6	−10	−70	572		184.8	190.9	−9.8	−71	790

(continued on next page)

Table 1 (continued)

Site Date	Depth, m Upper	Depth, m Lower	$\delta^{18}\text{O}$ (‰)	$\delta\text{D}$ (‰)	EC ( $\mu\text{S}/\text{cm}$ )	Site Date	Depth (m) Upper	Depth (m) Lower	$\delta^{18}\text{O}$ (‰)	$\delta\text{D}$ (‰)	EC ( $\mu\text{S}/\text{cm}$ )
M2 (TH76B)	298.5	304.5	-10.1	-71	992	January-2003	206.1	212.1	-10.1	-74	800
	330.3	336.4	-10.4	-73	1190		237.9	243.9	-9.9	-71	960
	306.1	312.1	-10.7	-78	6670		M5 (FBT-3)	148.5	154.5	-10.1	-71
366.7	372.7	-10.0	-73	10,060	163.6	169.7		-10.0	-71	2110	
418.2	424.2	-10.3	-74	16,630	181.8	187.9		-10.1	-72	1789	
January-05	472.7	478.8	-10.2	-74	19,280	December-2002	197.0	203.0	-10.3	-73	1775
	539.4	545.5	-9.2	-69	15,280		227.3	233.3	-10.4	-75	5290
	593.9	600.0	-9.5	-72	35,400		242.4	248.5	-10.3	-74	7660
M3 (TH 505A)	169.7	175.8	-10.4	-75	1458	M6 (DMW11)	275.8	281.8	-9.9	-71	12,070
	190.9	197.0	-10.6	-76	2300		290.9	297.0	-9.7	-71	15,300
	218.2	224.2	-10.5	-77	4080		136.4	142.4	-10.3	-73	2420
May-2005	239.4	245.5	-10.6	-76	5810	November-2002	163.6	169.7	-10.5	-76	2300
	300.0	306.1	-10.3	-73	10,150		233.3	239.4	-9.9	-71	970
	163.0	169.1	-10.5	-73	2750		257.6	263.6	-9.6	-68	1120
M4 (TH510A)	190.9	197.0	-10.5	-75	5240	June-2005	272.7	278.8	-9.5	-69	16,700
	215.2	221.2	-10.2	-76	6030		163.0	169.1	-10.5	-73	2750
	251.5	257.6	-10.2	-75	9240		190.9	197.0	-10.5	-75	5240
June-2005	275.8	281.8	-10.2	-74	12,110	June-2005	251.5	257.6	-10.2	-75	9240
	301.8	307.9	-9.9	-71	18,100		275.8	281.8	-10.2	-74	12,110
							301.8	307.9	-9.9	-71	18,100

aquifer is generally fresh on the western side of the basin, in the thickest part of the Camp Rice Formation. Prior to development, groundwater in the Hueco Bolson aquifer flowed south toward the study area. Pumping beneath El Paso and Ciudad Juárez has generated large cones of depression, and greatly modified the pre-development flow regime (Hibbs et al., 1997).

### 2.3. Previous isotope studies

Isotope data for municipal wells in the study area have been published by Eastoe et al. (2008) and Anderholm and Heywood (2002). Eastoe et al. (2008), summarizing data for a wide area of the Hueco Bolson, identified four types of groundwater on the basis of O and H isotopes. Three of the types, A, B and C, occur in western part of the Hueco Bolson. Type A originated as Rio Grande water, and represents mixtures of pre-dam and post-dam water. Type B also originated in the Rio Grande, and represents pre-dam river water. Type C is Hueco Bolson groundwater that originated as local precipitation that recharged along the Franklin and Organ Mountains, and has a wide range of  $\delta^{18}\text{O}$  and  $\delta\text{D}$  values thought to reflect differences in the isotope composition of precipitation as a function of age on the basis of the relationship between  $^{14}\text{C}$  and  $\delta^{18}\text{O}$  data (Eastoe et al., 2008). Dadakis (2004) mapped stable isotope and salinity variation in the Rio Grande alluvial aquifer from El Paso to Fort Quitman, finding type A water predominant nearer to El Paso, and type B water nearer to Fort Quitman. Druhan et al. (2008) mapped stable isotope and salinity layering in the Hueco Bolson aquifer immediately north of the present study area.

### 2.4. Previous modeling studies

The US Geological Survey developed the most recent ground water flow model of the Hueco Bolson (Heywood and Yager, 2003). The model code used was a modified version of MODFLOW-96, the modular finite-difference ground water flow model developed by the US Geological Survey (Harbaugh and McDonald, 1996). As described in Heywood and Yager (2003), the STR (streamflow-routing) and MAW (multi-aquifer well) packages were modified in order to deal with the large magnitude of historic drawdown that has been observed in the area, and the consequential issue of dried model cells in the upper layers of the model. The MAW package was previously developed by McDonald (1984), and

is not included as part of MODFLOW-96 as distributed by the USGS. The model grid consists of 10 layers of 165 rows and 100 columns in a variable grid ranging from 500 m by 500 to 1000 m by 1000 m, with the finer grid in the area of interest near El Paso and Juárez. The 10-layer vertical discretization of the flow system provides an opportunity to evaluate vertical flow in the system (i.e. flow between layers).

Heywood and Yager (2003) calibrated the model, using data from 1903 to 1996, by adjusting parameter values representing aquifer properties and specified boundary conditions using nonlinear regression techniques to minimize the difference between measured data and model-estimated data. Calibration relied on comparisons between actual and estimated ground water elevation data and selected surface water flows. More recently, El Paso Water Utilities updated the model to include input data from 1997 to 2002 (Hutchison, 2006). Hutchison and Hibbs (2008) applied the model to an analysis of cross-formational groundwater flow in the Hueco Bolson, delineating zones in which pumping since 1903 has reversed or enhanced the flow of water between river alluvium and the deeper regional aquifer.

## 3. Methods

At all sites except R7, the test holes were drilled to full depth, and then progressively back-filled with gravel. Intervals yielding water were isolated with bentonite plugs above and below, and sampled by lifting water from between the plugs in a stream of compressed air. Samples were accepted once electrical conductivity (EC) and pH had stabilized. Minimal evaporation is expected because a given volume of water is exposed to only enough air to carry it to the surface. The sampling method is not considered to be appropriate for carbon-14 analysis because of the high likelihood of addition of atmospheric  $\text{CO}_2$  to the sample from the compressed air. Samples from site R7 (Fig. 1) were collected from a US Geological Survey well nest after purging three volumes from each casing. The sample set differs from earlier data sets from the area in being specific to depth intervals of 6 m or less in most cases, as opposed to the much longer screens of municipal wells.

Specific electric conductivity (EC) was re-measured in the laboratory; these are the values reported here. Stable O and H isotopes were measured on a Finnigan Delta S mass spectrometer equipped with a Finnigan automated  $\text{CO}_2$  equilibrator for O, and a Finnigan

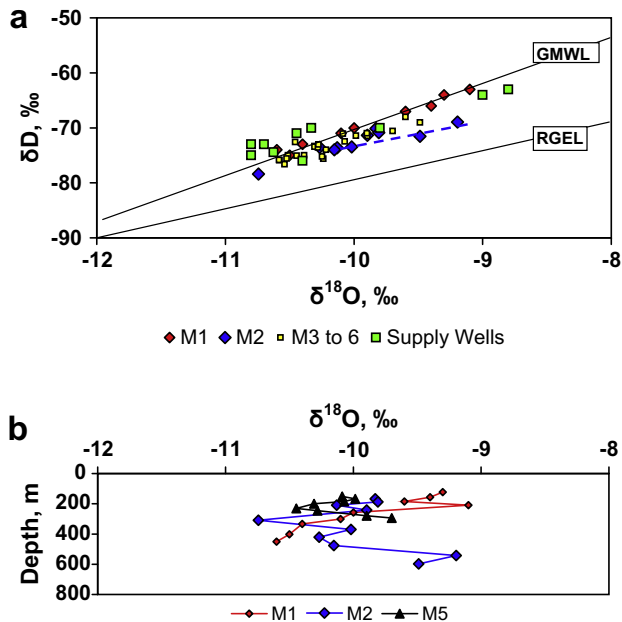


**Fig. 3.** (a) Plot of  $\delta D$  vs.  $\delta^{18}O$ , showing data from the mesa traverse and from nearby municipal supply wells. GMWL = global meteoric water line (Craig, 1963). RGEL = Rio Grande evaporation line, from data of Phillips et al., 2003). The dashed line is the suggested evaporation trend for site M2. (b) Plot of depth below surface vs.  $\delta^{18}O$  for certain mesa section samples. Points are linked in order of depth.

automated H/Device using metallic Cr as a reductant for H. Analytical precisions ( $1\sigma$ ) are  $0.08\text{‰}$  for O, and  $0.9\text{‰}$  for H.

#### 4. Isotope and salinity data

Data from all sites are listed in Table 1. For purposes of analysis and discussion the dataset is split into two cross sections. The “river traverse” follows the Rio Grande roughly NW to SE and includes wells drilled within the floodplain. The “mesa traverse” parallels the river traverse on higher ground 5–10 km from the river.

##### 4.1. Mesa traverse

On a plot of  $\delta D$  vs.  $\delta^{18}O$  (Fig. 3a) mesa groundwater samples plot as type C water and exhibit a wide range of salinities (EC span  $500\text{--}36000\ \mu\text{S cm}^{-1}$ ). The range of data ( $\delta^{18}O$  between  $-8.8$  and  $-11.0\text{‰}$ ) is similar to that for type C water obtained from supply wells (Eastoe et al., 2008), but there are more data on the right-hand side of the global meteoric water line (GMWL) indicating evaporation. The data set of Eastoe et al. (2008) included only data for potable water with low salinities, whereas the test holes sampled for this study yielded more saline water showing isotope effects of evaporation in many cases.

Data from two contrasting sites help to illustrate these differences. Waters from site M1, within the Franklin Mountains freshwater lens, originated from the ranges bounding the Hueco Bolson to the west (Hibbs et al., 1997). Isotope data plot along the GMWL, and the observed decrease of  $\delta^{18}O$  with depth is explained by increasing water age with depth, on the basis of the relationship between  $^{14}C$  and  $\delta^{18}O$  data for fresh water near the Franklin Mountains (Eastoe et al., 2008). At site M2, the data plot on an evaporation trend (Fig. 3a), and values of  $\delta^{18}O$  decrease with depth to about 300 m below the surface, and then increase with depth below 300 m (Fig. 3b). The deepest samples are the most

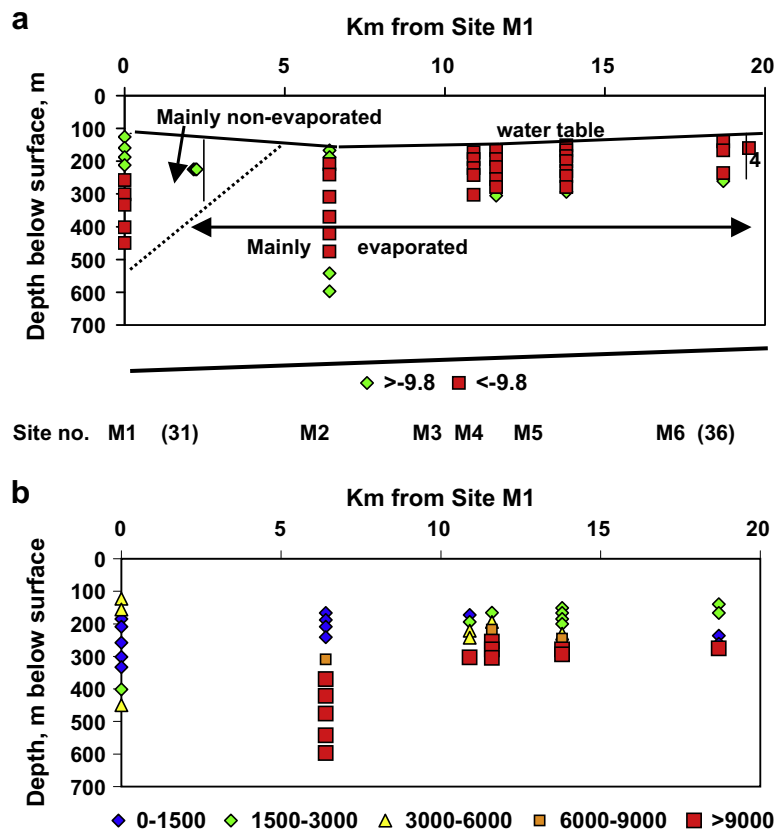


**Fig. 4.** Vertical sections along the mesa traverse. (a)  $\delta^{18}O$  data, with a dashed line showing the approximate boundary between non-evaporated and evaporated groundwater. The datum for the depth axis is the surface; the actual surface slope is shown by the heavy oblique line beneath the figure. (b) Specific electric conductivity data,  $\mu\text{S/cm}$ .

evaporated. Isotope–depth relationships at sites M3–M6 are similar to those at M2, but the inflection of the  $\delta^{18}\text{O}$  profiles occurs at shallower depths. Similar patterns were described in sets of vertical zone samples from the Hueco Bolson to the north of this traverse (Druhan et al., 2008).

The vertical profile along the traverse shows isotope layering (Fig. 4a, in which the data threshold at  $\delta^{18}\text{O} = -9.8\text{‰}$  is arbitrary). The evaporated, high- $\delta^{18}\text{O}$  water at depth and at the east side of the traverse are the most saline waters in the area (Fig. 4b), and may contain a fraction of connate water of lacustrine origin, or groundwater that has traveled south from the Tularosa basin in New Mexico (Druhan et al., 2008).

#### 4.2. River traverse

On a plot of  $\delta^{18}\text{O}$  vs.  $\delta\text{D}$  (Fig. 5a), the entire isotope data set plots within or between fields A, B and C of Eastoe et al. (2008). EC values range from 600 to 30,600  $\mu\text{S cm}^{-1}$ . None of the data set plots in the high- $\delta^{18}\text{O}$  end of field C observed for the mesa traverse. On the basis of  $\delta^{18}\text{O}$  vs.  $\delta\text{D}$  plots, groundwater can be classified as type A, B or C, or mixtures. Samples classified as type A waters plot close to the Rio Grande evaporation line (RGEL) at high  $\delta^{18}\text{O}$  values and are easily identified. In contrast samples classified as types B and C have similar  $\delta^{18}\text{O}$  values and plot close to the Rio Grande evaporation line (RGEL) and the GMWL, respectively.

Identifying mixtures of water types presents a challenge. Mixtures should plot along straight lines between end-members in Fig. 5. B + C mixtures are to some extent masked by the small isotope differences between the two end-members; they are most easily distinguished in plots for individual wells (e.g. Figs. 5b and c) where they are shifted to higher  $\delta^{18}\text{O}$  and  $\delta\text{D}$  values relative to type B water. These mixtures appear to combine type B water with high- $\delta^{18}\text{O}$  type C water that may belong to an evaporation trend like that of site M2 of the mesa traverse (Fig. 3a). This interpretation makes better spatial sense than for the samples in question to be A + low- $\delta^{18}\text{O}$  C mixtures, as can be seen in Fig. 6; mixtures containing type A water are likely to be found only near the surface. An evaporation trend like that at M2 may in fact be present in the river traverse data (Fig. 5a), but could also be explained as mixtures of low- $\delta^{18}\text{O}$  type C water with type A water. Again, spatial distribution (Fig. 5a) suggests that C + A mixing is reasonable for one sample at site R8 (79 m), and possibly 4 samples at site R11; the remaining examples are remote from type A water and are therefore B + evaporated C mixtures. Two examples of B + A mixtures were identified from the isotope data.

Mixing is also suggested by the lack of correlation between salinity and water type boundaries as shown in Fig. 6. Mixing is in fact more complex than suggested by Fig. 6, involving also type A water to a depth of 175 m at site R7, on the evidence of tritium content (Hutchison and Hibbs, 2008).

Isotope stratification is clearly present in groundwater of the river traverse and varies systematically along the length of the traverse. For wells close to the river (Fig. 6a) a layer of type A water is present from the surface down to 80 or 100 m, but may be absent at the most westerly sites (R2–R4); however no water samples were collected above 70 m. Below this layer occurs a layer of type B water up to 230 m thick. The layer is thickest between 0 km and 7 km (Fig. 6a), where river water has recharged the Hueco Bolson aquifer to depths exceeding 300 m. Between 7 and 12 km this layer thins and ultimately is not present at sites R8 and R9. Underlying the type B water is a layer that consists of type C water, or B + C mixtures of the types discussed above. A single exception to the general pattern is observed at site R2, where one sample of B + C mixture was found above the layer of type B water. This may be due to local leakage from the municipal water system.

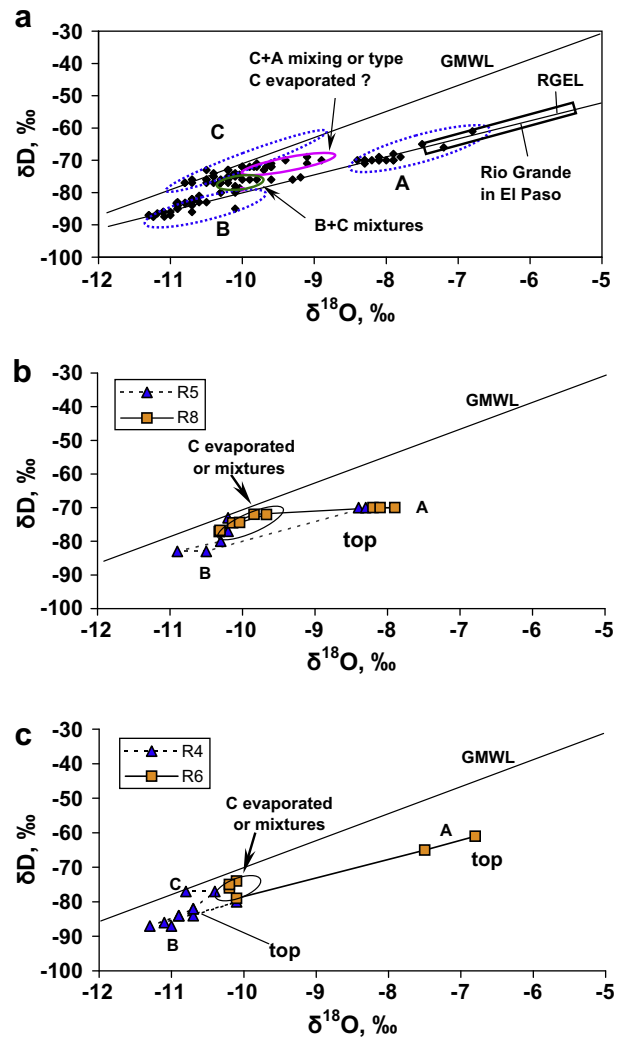


Fig. 5. Plots of  $\delta\text{D}$  vs.  $\delta^{18}\text{O}$ , showing data groupings (A, B, C and Rio Grande surface water in El Paso) of Eastoe et al. (2008), and isotope data from the river traverse. (a) All data from this study; (b) data for test holes R5 and R8, with points linked in order of depth. GMWL = global meteoric water line (Craig, 1963); and (c) data for test holes R4 and R6. RGEL = Rio Grande evaporation line, from data of Phillips et al., 2003).

For wells further from the river, but still within the floodplain, there is a shift in isotopic stratification with type C water at shallower depths. At site R12 (Fig. 6c), type A water overlies type C to a depth of at least 73 m. At R11, the water to a depth of 179 m may be A + C or B + evaporated C mixtures, with the exception of one sample of B + C at 149 m. Low salinity in the upper part of R11 suggests the presence of A + C mixtures.

In the salinity sections (Figs. 6b and 6d), all water with EC greater than 6000  $\mu\text{S cm}^{-1}$  is type C water or B + C mixtures. EC generally increases with depth beneath the 6000  $\mu\text{S cm}^{-1}$  boundary (Table 1). Above that boundary, which does not coincide with the B/B + C mixture isotope boundary, salinity varies non-uniformly with depth.

#### 4.3. Tritium and carbon-14

Data are available only for the well nest at site R7 (Hutchison and Hibbs, 2008) and for supply wells in the area of the two traverses (Table 2, including data from Eastoe et al., 2008). In general, tritium is below detection; four exceptions with 1.6 TU or less indicate local additions of recent rainwater or river water. The

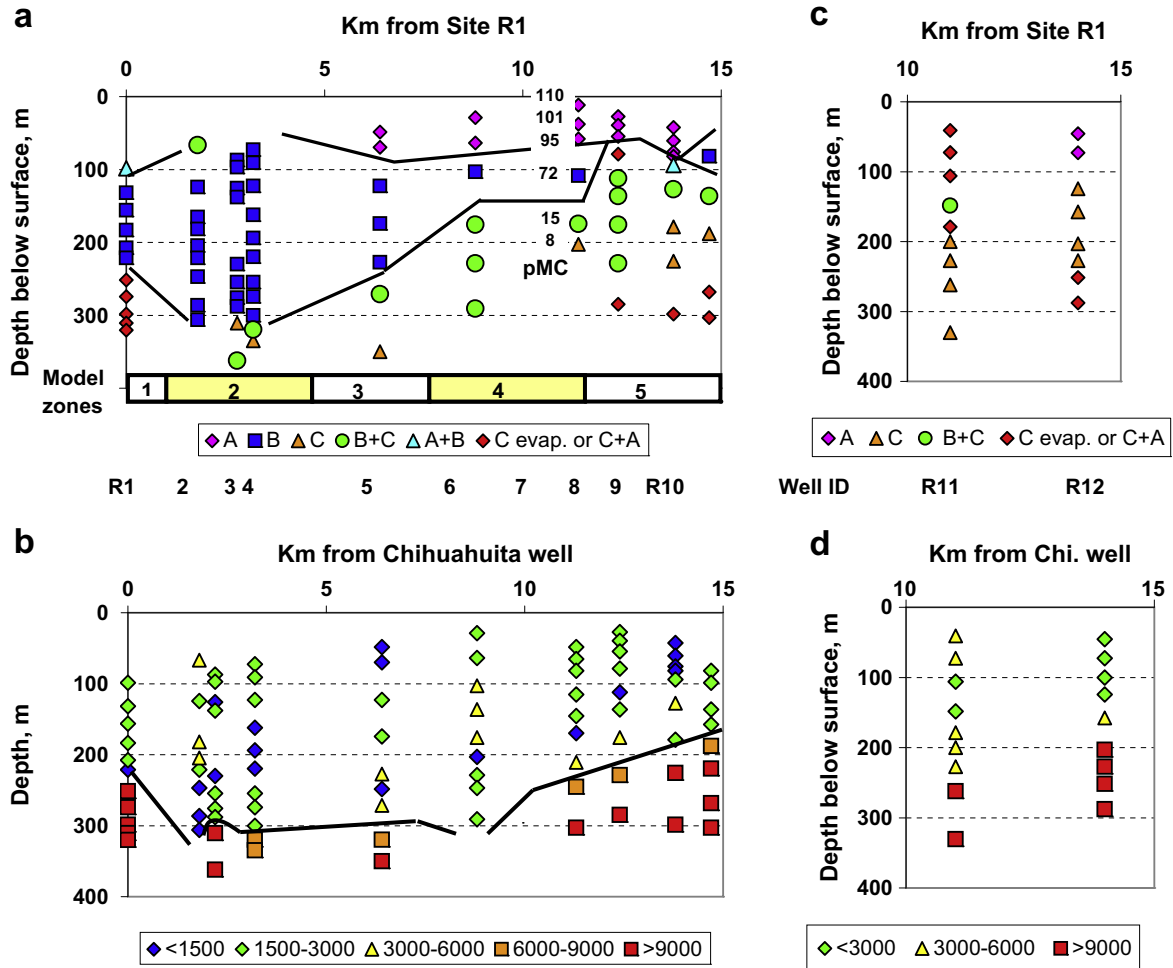


**Fig. 6.** Vertical sections of the river traverse showing sample locations, classified in terms of isotope data groups of Fig. 5 (panels a and c), and specific electric conductivity,  $\mu\text{S}/\text{cm}$  (panels b and d). Panels a and b show data for sites R1–R10 close to the Rio Grande. Panels c and d show data for test holes R11 and R12, in the flood plain northeast of the Rio Grande. The datum for the depth axis is the surface; between R1 and R10 the surface altitude decreases by 20 m.  $^{14}\text{C}$  content is given for samples at site R7. Model zones at the base of panel a are the intersections of zones shown in Fig. 7 with this section.

**Table 2**  
Tritium and C-14 data from supply wells near the study area.

Sample	Site no.	Screen m	$\delta^{18}\text{O}$	$\delta\text{D}$	C-14 pMC	Tritium TU
<i>Type B water</i>						
EPWU well 9	S7	140–291	–11.5	–85	29.7	<0.5
EPWU well 14	S8	146–291	–11.2	–85	55.2	1.2
EPWU well 408	S23	130–230	–10.9	–82	59.8	1.6
EPWU well 414	S24	346–530	–11.2	–82	28.1	<0.5
<i>Type C water</i>						
Vista Hills Blue well	S4		–10.8	–75	5.7	<0.5
Well 2 Vista Hills	S5		–10.8	–73	5.4	<0.6
EPWU well 45	S14	95–252	–10.3	–70	5.8	<0.9
EPWU well 63	S17	121–240	–10.4	–71	6.5	0.5
EPWU well 69	S18	114–164	–10.7	–73	7.1	<0.4
EPWU well 420	S26	136–192	–10.6	–74	10.2	<0.6
Fort Bliss 7	S31		–9.8	–70		<0.5
Intl. Garment Proc. 4	S36	118–215	–10.4	–76	3.8	1.1

EPWU = El Paso Water Utilities.  
Data from Eastoe et al. (2008).

presence of tritium is not accompanied by significant stable isotope shifts, suggesting addition of small amounts of high-tritium water at the peak of the tritium bomb pulse. Carbon-14 ranges at site R7 are 95–110 pMC for type A water; 28–75 pMC for type B water,

and 4–5 pMC for type C and B + C mixtures. Type C water from supply wells north of the flood plain generally contains 4–7 pMC.

## 5. Subregional groundwater budgets

The results of a groundwater flow model of the area were used to assist in the interpretation of the results of the isotopic analyses. Subregional groundwater budgets were developed using ZONE-BUDGET (Harbaugh, 1990) from model output to track changes in flow patterns and amounts in each of five areas defined on the basis of the isotopic analyses (Fig. 7; also see Fig. 6 for the relationship of the zones and the isotope data). The analysis grouped model layers into four vertical groups: The shallowest portion represents the uppermost 100 m (approximately), and includes model layers 1–3. Layers 4–6 represent the next 100 m (approximately). The next 90–100 m includes model layers 7–9. The deepest portion thickens from about 20 m in Zone 1 to nearly 250 m in Zone 5 and coincides with model layer 10.

### 5.1. Pre-development flow conditions

Fig. 8 summarizes the subregional groundwater budgets for the year 1903, and represents pre-development and pre-dam conditions. In Zone 1, all water that was recharged flowed down and to

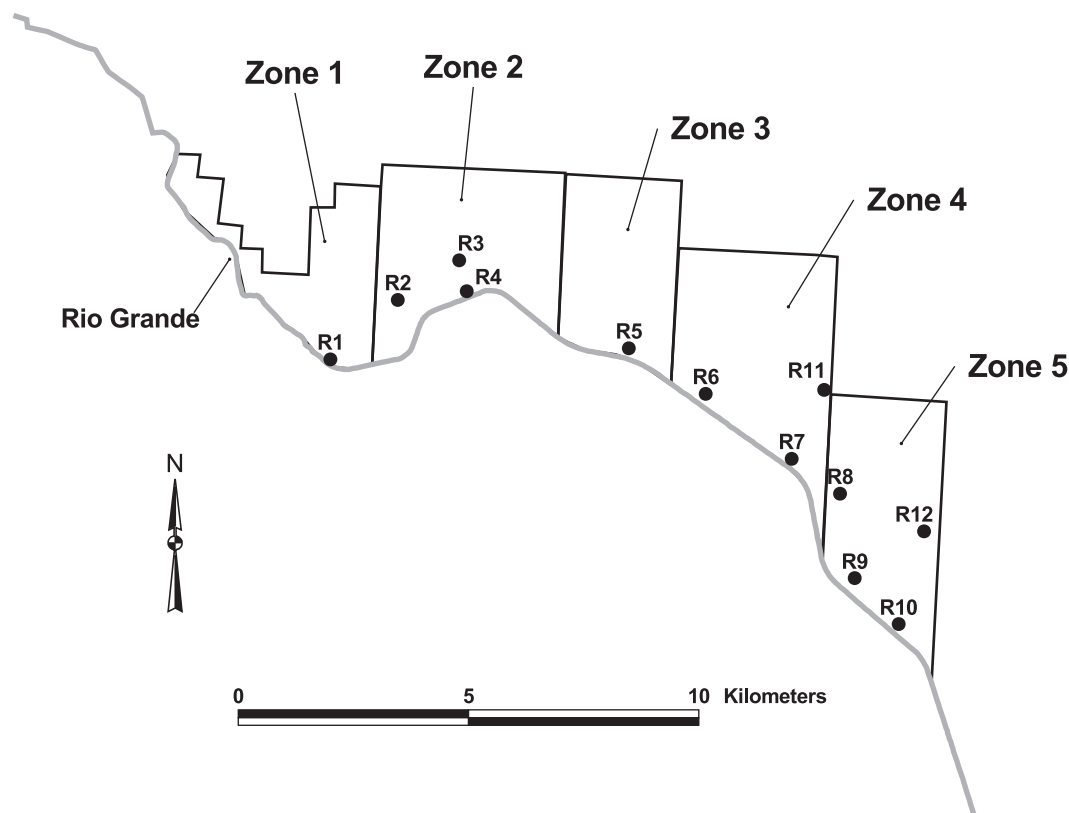


Fig. 7. Location of subregional water budget zones and location of sampling sites. See Fig. 6 for the relationship of the zones to the isotope data.

Juárez (south) and west (down the axis of the Rio Grande) into Zone 2. Inflow into Zone 2 was generally from Zone 1 and from El Paso. The shallowest section also received inflow from Juárez. In this shallow zone, there was a net discharge of  $1658 \text{ m}^3/\text{day}$  into the Rio Grande. Discharge from Zone 2 was down the axis of the Rio Grande and, in the deeper portions, to Juárez. In Zone 3, flow was generally from Zone 2 and from El Paso, and outflow is generally to Juárez. Note also that between Zones 1 and 3, vertical flow transitioned from downward in Zone 1 to upward into the shallow portions and downward in the deeper portions of Zones 2 and 3. The vertical gradient was upward in both Zones 4 and 5, and there was a net discharge to the Rio Grande in both of these zones. Lateral inflow to Zone 4 was from Zone 3, and El Paso. Lateral outflow from Zone 4 was to Zone 5 and to Juárez. In the upper 187 m of Zone 5, lateral inflow was from Zone 4 and Juárez, and lateral outflow was to El Paso. Below 187 m, lateral inflow was from Zone 4, and lateral outflow was to both El Paso and Juárez. In general, it can be seen that type B water would be expected to have been dominant in Zones 1 and 2. Type B water would likely have been dominant in upper Zone 3, and type C in lower Zone 3, with a possibility of some mixing. Type C water would have dominated in Zones 4 and 5.

### 5.2. Post-development flow conditions

In 1968, pumping in El Paso was higher than in Juárez. In general, this pumping tended to induce flow from Juárez to El Paso (Hutchison and Hibbs, 2008). To the extent that type B water had moved into Juárez under pre-development conditions, the reversal caused by pumping would have tended to result in mixing type B water with type C water. Post-dam river water, present only since 1916, recharged the upper layer and mixed with type B water to yield type A water. Fig. 9 summarizes the subregional groundwater budgets in 1968. Fig. 10 summarizes subregional groundwater

budgets in 2002 when Juárez pumping was higher than El Paso pumping. This condition has resulted in a general inducement of groundwater flow from the El Paso area into Juárez. This inducement has resulted in a combination of further mixing and the movement of type C water into areas that had once been dominated by type A or B water. Most of the wells in the area are screened across several layers and intraborehole flow is estimated by the MAW package. Zinn and Konikow (2007) demonstrated the potential effect of intraborehole flow by completing numerical experiments on a hypothetical, anisotropic, homogenous aquifer system with long-screened wells. Mixing associated with intraborehole flow was found to be dependent on the location of the borehole within the system, the local head gradients, and temporal factors. Thus, the post-development movement and mixing can be attributed to both vertical flow in the aquifer system and intraborehole flow due to the screen location across several layers.

### 5.3. Present flow conditions

Of particular importance in this analysis is the interpretation of 2002 subregional groundwater budgets (Fig. 10). Due to the relatively stable pumping regime from 2002 to 2006, the 2002 subregional groundwater budgets are considered representative of the conditions present when the samples were collected. In contrast to pre-development conditions (Fig. 8), groundwater in all zones is generally moving from El Paso, through the five zones along the Rio Grande, and into Juárez. Also of note is the reversal in movement along the axis of the Rio Grande. During pre-development conditions, flow generally moved down the axis of the Rio Grande (from Zones 1 to 5). Under 2002 conditions, groundwater flow was from Zones 5 to 1. Thus, the dominance of type C water or B + C mixtures at depth from R6 to R10 is due to the inducement of El Paso water into the study area as it moves into Juárez as a

Year 1903

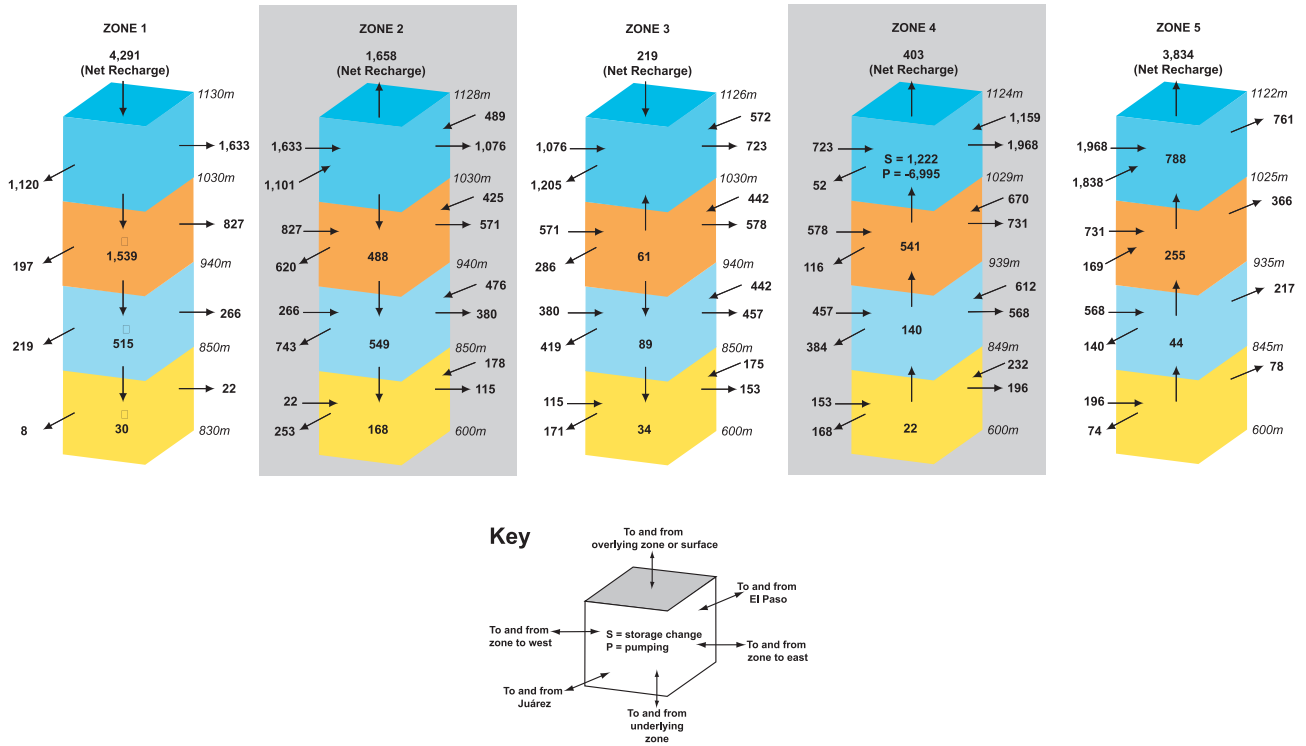


Fig. 8. Subregional groundwater budget under pre-development conditions (1903). Inflows are designated as arrows into the blocks; outflows are depicted as arrows out of the blocks. Elevations of the four depth zones are shown on the blocks. All values in m<sup>3</sup>/day.

Year 1968

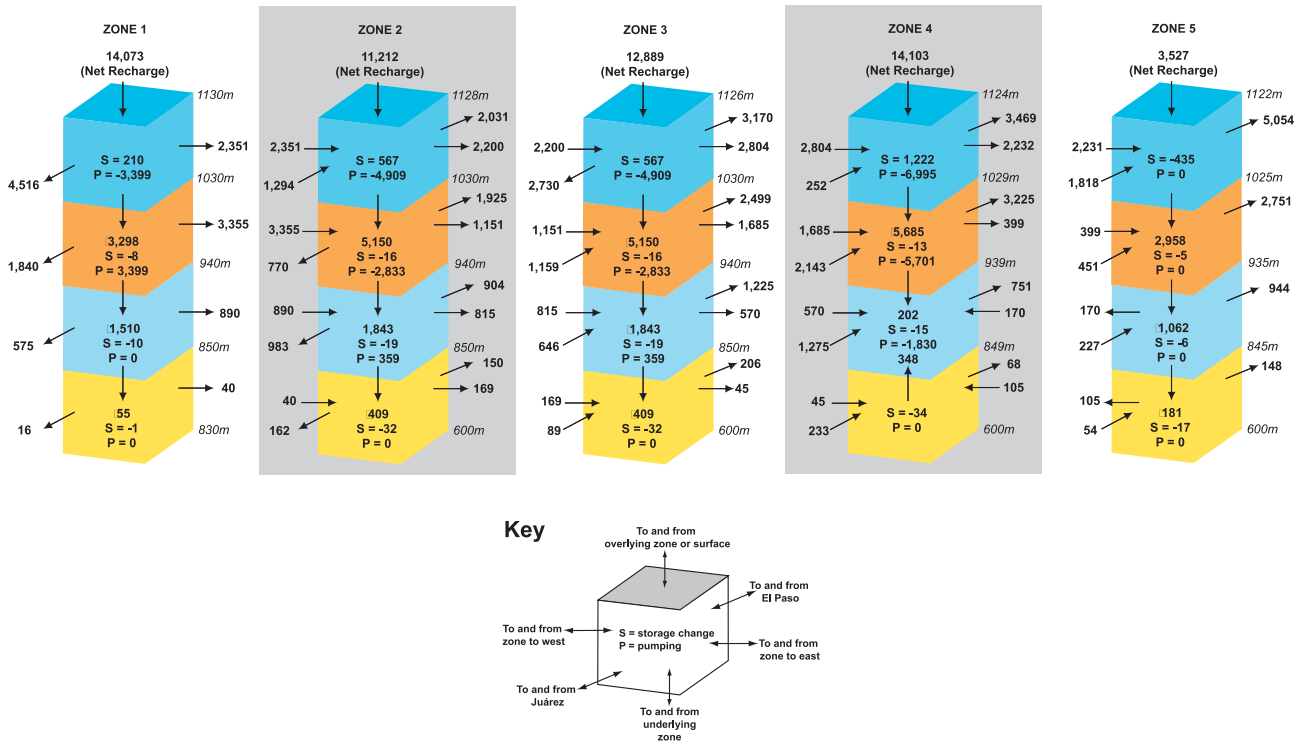
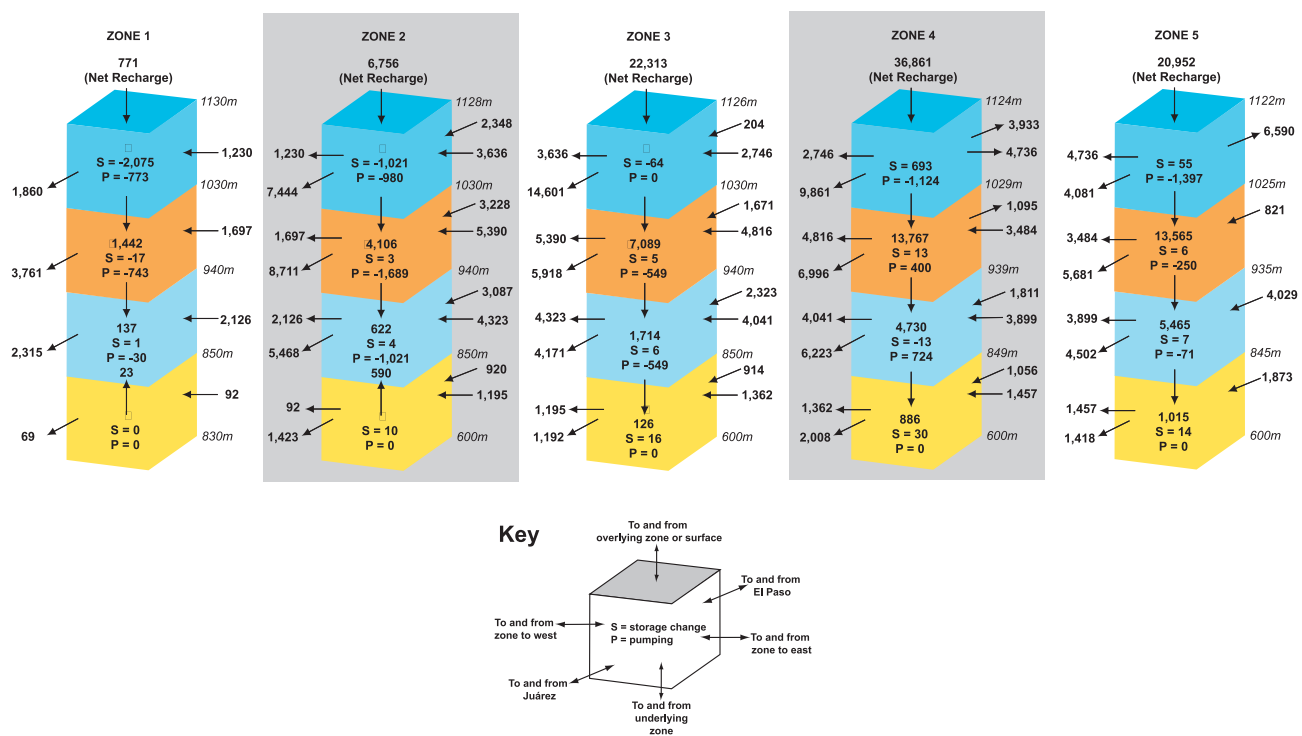


Fig. 9. Subregional groundwater budget under transient conditions in 1968. Inflows are designated as arrows into the blocks; outflows are depicted as arrows out of the blocks. Negative pumping estimates represent discharge from the area, and positive estimates represent inflows to the area. Negative storage changes represent storage declines and positive storage changes represent storage increases. Elevations of the four depth zones are shown on the blocks. All values in m<sup>3</sup>/day.

## Year 2002



**Fig. 10.** Subregional groundwater budget under transient conditions in 2002. Inflows are designated as arrows into the blocks; outflows are depicted as arrows out of the blocks. Negative pumping estimates represent discharge from the area, and positive estimates represent inflows to the area. Negative storage changes represent storage declines and positive storage changes represent storage increases. Elevations of the four depth zones are shown on the blocks. All values in  $\text{m}^3/\text{day}$ .

result of pumping-induced gradients. The large type B zone of R2–R4 does not correspond well with the 2002 model, but rather appears to represent recharge of river water under pre-development conditions (Fig. 8) with little or no indication of mixing with type C water.

## 6. Discussion

### 6.1. Comparison of model predictions and isotope data

The subregional water budget model and the isotope profile are two independent means of tracing the flow of groundwater in the study area. They differ in one important respect; modeling represents the state of an aquifer at a particular time, whereas isotope distribution reflects the integrated effects of long-term flow and mixing. In the present study, the two approaches agree in several important ways: (1) the presence of the layer of type A water over much of the study area; (2) the presence of B + C mixtures in Zones 3–5; and (3) the abundance of unmixed type C water in Zone 5. The B + C mixing in Zones 3–5, shown indistinctly by the isotope data, is confirmed by the model inasmuch as the model shows a change of flow direction over time in those zones.

In other respects, the model predictions and the isotope data show at best partial agreement: (1) the lack of mixing of water types B and C to a depth of 300 m in Zone 2 corresponds to 1968 model conditions, but not to 1903 or 2002 conditions; (2) the apparent absence of type A water, and the presence of an apparent mound of type B water, in upper Zone 2 is not predicted under 1968 or 2002 conditions, but is consistent with 1903 conditions. Such partial mismatches between the isotope profile models may illustrate the tendency of isotopes to provide a longer-term view of groundwater flow in comparison to modeling – deep infiltration in Zone 2 will be discussed below.

A more quantitative comparison of the modeling and the isotope data is not possible. A mass-balance calculation of isotope composition in B + C mixtures using modeled flows between the zones and layers of Figs. 7–10 fails to yield meaningful results because type B and C waters, while recognizable according to isotopes, do not each have a single isotope composition that can be used as an end-member for the purposes of calculation. Furthermore, the model requires the addition of B + C mixture of unknown composition (Fig. 10, Zone 4).

### 6.2. Origin of saline type C water in the river traverse

The type C water encountered in the river traverse is of very high salinity, and varies in degree of evaporation according to the isotope data. Values of  $\delta^{18}\text{O}$  in less-evaporated examples are  $< -10\%$ . Such water matches the water mapped at depth from site M2 to site M6 along the mesa traverse. Sites R8 and R11, where type C water or B + C mixtures have largely displaced unmixed type B, appear to lie near the focus of a zone of discharge of type C water into the shallow aquifer. Low-salinity type C water with  $\delta^{18}\text{O} > -10\%$  and plotting along the GMWL (as at site M1, and as found by Eastoe et al., 2008, in production well samples) is absent in the river traverse sample set. The freshest groundwater of the Hueco Bolson is of this type. Such water is not at present being discharged to the flood plain sediment in the study area, most likely because pumping in the upgradient area to the north has supplanted natural discharge.

An unexpected result of the study is the presence of evaporated type C water at site R1; this site is at the western end of a basin embayment, an volume of sediment that is shielded from the basin fill to the northeast and east (where evaporated type C water prevails) by the hard rock of the Franklin Mountains, and by a large volume of basin fill in which river water infiltrates to a depth of 300 m.

### 6.3. The dam-related isotope effect as a dating tool

The isotope signatures of pre-dam and post-dam river water are clearly visible in isotope layering in groundwater beneath the Rio Grande. The boundary surface at the base of the post-dam water in Zones 3–5 is a time marker above which river water has infiltrated since the construction of Elephant Butte dam in 1916, and below which little post-dam water has penetrated (the presence of a little tritium in the subjacent layers notwithstanding; local preferential flow presumably conveys small amounts of post-dam water to greater depths). In this way, stable O and H isotopes provide a dating tool applicable in Rio Grande basins downstream of the dam. Similar phenomena are likely in other arid or semiarid river basins with large dams, e.g. El Bakri et al. (1992).

### 6.4. Deep infiltration in Zone 2

Zone 2 lies within the narrow but deep embayment of basin-fill sediment between the Franklin Mountains and the Sierra de Juárez. The hard rock shields this volume of sediment from groundwater flow from the basin to the north, and river water infiltrates to the base of the Camp Rice formation (compare Figs. 2 and 6). Deep infiltration in the Camp Rice formation is consistent with high hydraulic conductivity in that formation. Direct measurements do not exist in the study area. Values of 4–7 m/day were used in the model used here, contrasting with a value of 0.9 m/day for the uppermost Fort Hancock formation. For comparison, Heywood and Yager (2003) cited a mean hydraulic conductivity of  $10 \pm 7$  m/day for Camp Rice formation sediment in the region. The vertical gradient of head at site R7, where a well nest is available, is downward (Hutchison and Hibbs, 2008), consistent with downward infiltration of type B water in that area; similar conditions may exist at sites R2–R5 where the isotope data show deeper infiltration, but no direct measurements of hydraulic gradient exist. Two possible explanations for such deep infiltration can be suggested: (1) several decades of pumping from municipal wells to 300 m depth in zone 2; or (2) replenishment of the Hueco Bolson aquifer to similar depths beneath Ciudad Juárez, providing an “escape” path for the water to the southeast, through ancestral Rio Grande channel deposits. In possible support of alternative 1, Pérez-Santiago (1997) found evidence for drawdown of the shallow aquifer near sites R2–R4 – but the boundary between type A and B water has not been drawn down in this area (Fig. 6a). In support of explanation 2, type B water also occurs in the Hueco Bolson aquifer beneath Ciudad Juárez (Eastoe et al., 2008), and is pumped from wells that extend to 251 m beneath the surface. It seems most likely that the deep infiltration of river water in the area of concern is a natural phenomenon, possible because the river water is able to flow to the southeast beneath Ciudad Juárez, through ancestral Rio Grande fluvial sediment that is present in that area to depths of 300 m (Fig. 2). The lack of mixing with type C water in this zone most likely reflects a smaller supply of type C water in Zone 2 than in Zones 3–5.

### 6.5. Geologic control of groundwater flow

The correspondence between the depth of infiltration of river water and the depth of ancestral Rio Grande fluvial sediments is striking. Eastoe et al. (2008) concluded that the distribution of such sediment controlled the flow of river-derived groundwater beneath Ciudad Juárez in plan view; this study shows that the same applies in the vertical dimension in the profile beneath the river. Preferential groundwater flow through ancient river channel deposits appears to be characteristic of alluvial aquifers of the Basin and Range, e.g. in Tucson Basin (Eastoe et al., 2004) and near Fabens in the Hueco Bolson (Hibbs et al., 2003).

### 6.6. Further work

The salinity profiles are complicated in type B and type B + C isotope zones. The complications may be explained by chaotic mixing of types B and C waters, or by supply of salt from clay aquitards that are present in the Camp Rice sediments beneath the river (Hutchison and Hibbs, 2008). More detailed chemical data, particularly chloride, sulfate and bromide analyses, were not gathered for this study, but might give additional insight on mixing.

## 7. Conclusions

Isotope and salinity stratification are present in groundwater to depths of 300 m in two profiles in basin fill of the Hueco Bolson. Stratification of O and H isotopes in native Hueco Bolson groundwater in a traverse on the mesas north of the Rio Grande reflects residence time and degree of evaporation. Stratification of O and H isotopes in a traverse along the Rio Grande is complex. Groundwater derived in part from the post-dam river (type A) overlies water from the pre-dam river (type B), but the latter is supplanted by or mixed with saline native Hueco Bolson groundwater (type C) in the downstream half of the traverse. Types C and A water mix locally within 100 m of the surface at the downstream end of the traverse. Low-salinity type C water, present at the western end of the mesa traverse, has not been observed in the river traverse.

The new data on geology and isotopes provide an unprecedented opportunity for comparing the results of MODFLOW modeling with field data. The isotope stratification along the river traverse is consistent with major predictions of flow modeling, in particular the pre-development interaction of type B water with type C groundwater, and post-development disturbances such as the construction of dams of the Rio Grande and pumping of water for municipal use. Flow modeling lends credence to the identification of groundwater mixing zones; where mixing of water types B and C appears to be prevalent, the modeling indicates a reversal of the flow direction of groundwater between El Paso and Ciudad Juárez as a result increased pumping under Ciudad Juárez. Flow modeling does not predict the infiltration (without mixing with type C) of type B water to 300 m in the upstream part of the river traverse under pre-development or current conditions. The modeling of water budgets and detailed isotope measurements complement each other in building an understanding of groundwater movement in the basin.

Several of the conclusions here should apply in general to river and alluvial basin systems, viz. the usefulness of the dam isotope effect, the importance of local geology as a factor governing recharge, the complexity of interaction between surface water and groundwater, and the satisfactory comparison between tracer and modeling studies.

## Acknowledgements

This material is based upon work supported by SAHRA (Sustainability of semi-Arid Hydrology and Riparian Areas) under the STC Program of the National Science Foundation, Agreement No. EAR-9876800, and by CEA-CREST (Center for Environmental Analysis, Centers for Research Excellence in Science and Technology) under National Science Foundation Cooperative Agreement No. HRD-0317772. The authors express gratitude to numerous well-owners who provided access and samples, notably El Paso Water Utilities, the United States Geological Survey, and the United States Army (Fort Bliss). The comments of anonymous reviewers enabled us to improve the manuscript greatly.

## References

- Anderholm, S.K., Heywood, C.E., 2002. Chemistry and Age of Groundwater in the Southwestern Hueco Bolson, US Geol. Surv. Water Res. Inv. Rep. 02-4237, New Mexico and Texas, 16 pp.
- Collins, E.W., Raney, J.A., 1994. Tertiary and Quaternary tectonics of the Hueco Bolson, Trans-Pecos Texas and Chihuahua, Mexico. In: Keller, G.R., Cather, S.M. (Eds.), Basins of the Rio Grande Rift-Structure, Stratigraphy and Tectonic Setting, vol. 291. Geol. Soc. America Special Paper, pp. 265–282.
- Connell, S.D., Hawley, J.W., Love, D.W., 2005. Late Cenozoic drainage developments in the southeastern Basin and Range of New Mexico, southeasternmost Arizona, and western Texas. In: Lucas, S.G., Morgan, G.S., Zeigler, K.E. (Eds.), New Mexico's Ice Ages, vol. 28. New Mexico Museum of Natural History and Science Bulletin, pp. 125–150.
- Craig, H., 1963. Isotopic variation in meteoric waters. *Science* 133, 1702–1703.
- Dadakis, J.S., 2004. Isotopic and Geochemical Characterization of Recharge and Salinity in a Shallow Floodplain Aquifer Near El Paso, Texas. Unpubl. M.S. Thesis, Univ. of Arizona, 102 pp.
- Druhan, J.L., Hogan, J.F., Eastoe, C.J., Hibbs, B., Hutchison, W.R., 2008. Hydrogeologic controls on groundwater recharge and salinization: a geochemical analysis of the northern Hueco Bolson Aquifer, El Paso, Texas. *Hydrogeol. J.* 16, 281–286.
- Eastoe, C.J., Gu, A., Long, A., 2004. The origins, ages and flow paths of groundwater in Tucson Basin: results of a study of multiple isotope systems. In: Hogan, J.F., Phillips, F.M., Scanlon, B.R. (Eds.), *Groundwater Recharge in a Desert Environment: The Southwestern United States*, Water Science and Applications Series, vol. 9. American Geophysical Union, Washington, DC, pp. 217–234.
- Eastoe, C.J., Hibbs, B.J., Granados Olivas, A., Hogan, J., Hawley, J., Hutchison, W.R., 2008. Isotopes in the Hueco Bolson Aquifer, Texas (USA) and Chihuahua (Mexico): local and general implications for recharge sources in alluvial basins. *Hydrogeol. J.* 16, 737–747.
- El Bakri, A., Tantawi, A., Blavoux, B., Dray, M., 1992. Sources of water recharge identified by isotopes in El Minya Governate (Nile Valley, Egypt). In: *Isotope Techniques in Water Resources Development 1991*. IAEA Symposium, vol. 319, Vienna, Austria, pp. 643–645.
- Harbaugh, A.W., 1990. A Computer Program for Calculating Subregional Water Budgets Using Results from the US Geological Survey Modular Three-dimensional Finite-difference Ground-water Flow Model. US Geol. Surv. Open-File Report 90-392.
- Harbaugh, A.W., McDonald, M.G., 1996. User's documentation for MODFLOW-96, an Update to the US Geological Survey Modular Finite-Difference Ground-Water Flow Model: US Geol. Surv. Open-File Report 96-485.
- Hawley, J.W., Kernodle J.M., 2000. Overview of the hydrology and geohydrology of the northern Rio Grande basin – Colorado, New Mexico and Texas. In: Ortega-Klett, C.T. (Ed.), *The Rio Grande Compact: It's the Law! Proceedings of the 44th Annual New Mexico Water Conference*, New Mexico Water Resources Research Institute Report, vol. 312, pp. 79–102.
- Heywood, C.E., Yager, R.M., 2003. Simulated Ground-water Flow in the Hueco Bolson, an Alluvial-Basin Aquifer System near El Paso, Texas. US Geol. Surv. Water-Resources Investigations Report 02-4108.
- Hibbs, B.J., Boghici, R.N., Hayes, M.E., Ashworth, J.B., Hanson, A.N., Samani, Z.A., Kennedy, J.F., Creel, R.J., 1997. Transboundary Aquifers of the El Paso/Ciudad Juárez/Las Cruces Region. Contract Report, Texas Water Development Board, Austin & New Mexico Water Resources Research Institute, Las Cruces, 148 pp.
- Hibbs, B., Eastoe, C., Dadakis, J., 2003. New insights on salinization and predevelopment recharge of the Rio Grande Aquifer. In: *El Paso/Juárez Area: 2003 Annual Meeting*, Geological Society of America, November 2003, Abs. with Programs, Paper 67-6.
- Hutchison, W.R., 2006. Groundwater Management in El Paso, Texas. Ph.D. Dissertation, The University of Texas at El Paso, 329 p.
- Hutchison, W.R., Hibbs, B.J., 2008. Ground-Water budget analysis and cross-formational leakage in an arid basin. *Ground-Water* 46, 384–395.
- McDonald, M.G., 1984. Development of a multi-aquifer well option for a modular ground-water flow model. In: *Proceedings of the National Water Well Association Conference, Practical Applications of Ground-water Models*, pp. 786–796.
- Pérez-Santiago, V., 1997. Heterogeneity and Water Quality in the Rio Grande Alluvium, Downtown El Paso, Texas, Unpub. M.S. Thesis, Univ. Texas El Paso, 137 pp.
- Phillips, F.M., Hogan, J., Mills, S., Hendrickx, J.M.H., 2003. Environmental tracers applied to quantifying causes of salinity in arid-region rivers: preliminary results from the Rio Grande, southwestern USA. In: Alsharhan, A.S., Wood, W.W. (Eds.), *Water Resources Perspectives: Evaluation, Management and Policy*. Elsevier Science, Amsterdam, pp. 327–334.
- Stuart, C.J., Willingham, D.L., 1984. Late Tertiary and Quaternary fluvial deposits in the Mesilla and Hueco Bolsons, El Paso area, Texas. *Sed. Geol.* 38, 1–20.
- Zinn, B.A., Konikow, L.F., 2007. Effects of interborehole flow on groundwater age distribution. *Hydrogeol. J.* 15, 633–643.